Pharmacokinetic and Metabolomic Studies with a Promising Radiation Countermeasure, BBT-059 (PEGylated interleukin-11), in Rhesus Nonhuman Primates

Authors: Carpenter, Alana D., Li, Yaoxiang, Wise, Stephen Y., Fatanmi, Oluseyi O., Petrus, Sarah A., et al.

Source: Radiation Research, 202(1) : 26-37

Published By: Radiation Research Society

URL: https://doi.org/10.1667/RADE-23-00194.1

RADIATION RESEARCH **202**, 26–37 (2024)
0033-7587/24 $15.00

DOI: 10.1667/RADE-23-00194.1

Pharmacokinetic and Metabolomic Studies with a Promising Radiation Countermeasure, BBT-059 (PEGylated interleukin-11), in Rhesus Nonhuman Primates

Alana D. Carpenter,[a,b,1] Yaoxiang Li,[c,1] Stephen Y. Wise,[a,b] Oluseyi O. Fatanmi,[a,b] Sarah A. Petrus,[a,b] Christine M. Fam,[d] Sharon J. Carlson,[d] George N. Cox,[d] Amrita K. Cheema,[c,e] Vijay K. Singh[a,b,2]

[a] Division of Radioprotectants, Department of Pharmacology and Molecular Therapeutics, F. Edward Hébert School of Medicine, Uniformed Services University of the Health Sciences, Bethesda, Maryland 20814; [b] Armed Forces Radiobiology Research Institute, Uniformed Services University of the Health Sciences, Bethesda, Maryland 20814; [c] Department of Oncology, Lombardi Comprehensive Cancer Center, Georgetown University Medical Center, Washington, DC 20057; [d] Bolder BioTechnology, Boulder, Colorado, 80301; [e] Department of Biochemistry, Molecular and Cellular Biology, Georgetown University Medical Center, Washington, DC 20057

Carpenter AD, Li Y, Wise SY, Fatanmi OO, Petrus SA, Fam CM, Carlson SJ, Cox GN, Cheema AK, Singh VK. Pharmacokinetic and Metabolomic Studies with a Promising Radiation Countermeasure, BBT-059 (PEGylated interleukin-11), in Rhesus Nonhuman Primates. Radiat Res. 202, 26–37 (2024).

BBT-059, a long-acting PEGylated interleukin-11 (IL-11) analog that is believed to have hematopoietic promoting and anti-apoptotic properties, is being developed as a potential radiation medical countermeasure (MCM) for hematopoietic acute radiation syndrome (H-ARS). This agent has been shown to improve survival in lethally irradiated mice. To further evaluate the drug's toxicity and safety profile, 12 naïve nonhuman primates (NHPs, rhesus macaques) were administered one of three doses of BBT-059 subcutaneously and were monitored for the next 21 days. Blood samples were collected throughout the study to assess the pharmacokinetics (PK) and pharmacodynamics (PD) of the drug as well as its effects on complete blood counts, cytokines, vital signs, and to conduct metabolomic studies. No adverse effects were detected in any treatment group during the study. Short-term changes in metabolomic profiles were present in all groups treated with BBT-059 beginning immediately after drug administration and reverting to near normal levels by the end of the study period. Several pathways and metabolites, particularly those related to inflammation and steroid hormone biosynthesis, were activated by BBT-059 administration. Taken together, these observations suggest that BBT-059 has a good safety profile for further development as a radiation MCM for regulatory approval for human use.

INTRODUCTION

Exposures to ionizing radiation are an increasing threat in the current geo-political scenario. These exposures can bring about a variety of damaging health consequences which correspond to the dose of radiation received (*1*, *2*). Accordingly, radiological/nuclear preparedness and radiation countermeasures (MCMs) are security issues for the individual as well as for the nation (*3–6*). Ionizing radiation exposures can result in different types of radiation injuries requiring diagnostic and therapeutic measures. The clinical progression of acute radiation syndrome (ARS) depends on the absorbed radiation dose and the tissues affected (*7*). Clinical manifestations of ARS in humans include hematopoietic ARS (H-ARS) (2–6 Gy), gastrointestinal ARS (GI-ARS) (>6 Gy), and neurovascular (>10 Gy) subsyndrome (*8*). Individuals exposed to radiation resulting in H-ARS and GI-ARS have been the focus for the development of MCMs, as the neurovascular subsyndrome is considered incurable. At this time, the United States Food and Drug Administration (U.S. FDA) has approved the use of seven agents for H-ARS (Neupogen, Neulasta, Udenyca, Stimufend, Ziextenzo, Nplate, and Leukine), all of which require post-exposure administration as these are radiomitigators (*9–22*). Neupogen, Neulasta, Udenyca, Stimufend, Ziextenzo, and Leukine stimulate the production of neutrophils while Nplate stimulates platelet production. MCMs used prior to exposure are known as radioprotectors. Radiomitigators are needed for the treatment of victims of radiological/nuclear events while radioprotectors are required for use by military and first responders. No radioprotector has yet been approved by the U.S. FDA, though there are several under development (*23–27*).

Interleukin 11 (IL-11) is a member of the IL-6 family which possesses well-characterized biological actions including stimulatory and maturational actions on megakaryocytopoiesis and thrombocytopoiesis, along with anti-inflammatory

[1] These authors contributed equally to this study.
[2] Corresponding author: Vijay K. Singh, Ph.D., Division of Radioprotectants, Department of Pharmacology and Molecular Therapeutics, F. Edward Hébert School of Medicine, Uniformed Services University of the Health Sciences, 4301 Jones Bridge Road, Bethesda, MD 20814; email: vijay.singh@usuhs.edu.

and cytoprotective effects on GI crypts and hematopoietic progenitors (*28*, *29*). This agent also belongs to the gp130 family of cytokines; IL-11 is the only member which acts on a homodimer of the ubiquitously expressed gp130 co-receptor. Responsiveness of cells is determined by the presence of the IL-11 receptor alpha which is present on the wide range of cells (*28*). Because of this, the possibility exists that certain cells may not be responsive to IL-11 due to the lack of the IL-11 receptor alpha expression (*30*). IL-11 is a drug (Neumega/Oprelvekin, Wyeth Pharmaceuticals Inc. Philadelphia, PA) currently in clinical use for chemotherapy-induced thrombocytopenia. Recombinant human IL-11's therapeutic efficacy for the above indications has also been investigated (*29*, *31*, *32*). The effects of rhuIL-11 on thrombocytopenia and neutropenia have been investigated preclinically using both small and large animal models of radiation injury (*33–36*).

BBT-059 is a long-acting PEGylated IL-11 analog created using site-specific PEGylation technology and modified with a single branched 40 kDa-PEG at a cysteine residue (PEG-*179C) incorporated at the protein's C-terminus. BBT-059 is believed to bring about its biological effects such as the ability to stimulate the production of platelets, red blood cells, and to a lesser extent neutrophils by binding and activating the IL-11 receptors on cells. Hematopoietic and anti-apoptotic effects on many cell types by IL-11 and BBT-059 may be important for improving survival after lethal irradiation in the murine model (*29*, *36–38*). Unlike FDA-approved growth factors for ARS, BBT-059 has been shown to improve radiation-induced neutropenia as well as thrombocytopenia (*37*, *38*). In addition, BBT-059 is being developed as a potential treatment for thrombocytopenia, myelodysplastic syndromes, bleeding disorders, and acute kidney injury associated with ischemia reperfusion injury (*39*).

This study was conducted to assess the pharmacokinetics (PK) and pharmacodynamics (PD) of varying doses of BBT-059 and the concomitant metabolic changes using a nonhuman primate (NHP) model. PK and PD studies are a necessary step in drug development that allow for the establishment of plasma target concentration ranges as well as dose-response relationships (*40*). Metabolomics studies were also performed to determine the various metabolites and pathways stimulated or inhibited by BBT-059 administration. Numerous prophylactic radiation MCMs under development have been used to study metabolomics, including amifostine (*41–44*), BIO 300 (*27*, *45*, *46*), Ex-Rad (*47*), and gamma-tocotrienol (*26*, *48–50*).

The study was performed with 12 NHPs; four animals each were administered either 37.5, 75, or 150 μg/kg of BBT-059. The NHP model is known as the gold standard of animal models for developing radiation MCMs following the U.S. FDA Animal Rule and also for identifying and validating biomarkers for radiation injury and MCM efficacy (*51*). Three doses of BBT-059 were evaluated for PK/PD and metabolomics. The results of this study suggest that BBT-059 induces short-term changes in metabolomic profiles and stimulates pathways related to inflammation and steroid hormone production with no adverse side effects observed.

MATERIALS AND METHODS

Experimental Design

The primary objective of this study was to investigate the PK/PD profile of BBT-059 in rhesus NHPs as well as the metabolomic changes induced by drug administration. A total of 12 NHPs, divided into three groups with four animals per group, received single subcutaneous (SC) doses of BBT-059. Three different doses of BBT-059 (37.5 μg/kg, 75 μg/kg and 150 μg/kg; injection volume based on body weight not to exceed 1.33 ml) were used. The doses of BBT-059 selected for this study were allometrically scaled from previous studies conducted in a murine model, which demonstrated promising preliminary results (*37*, *38*). In brief, we used allometric scaling to extrapolate doses from mice to NHPs using information provided in the FDA Center for Drug Evaluation and Research (CDER) document (*52*). The PK/PD experiments in this study used the dose of 0.075 mg/kg, a twofold lower dose of 0.0375 mg/kg, and a twofold higher dose of 0.150 mg/kg. It has been reported that a single SC injection of 1.2 mg/kg BBT-059 in mice was safe (*37*). A dose of 1.2 mg/kg in mice is equivalent to a dose of 0.3 mg/kg for NHPs using allometric scaling, so the highest 0.15 mg/kg dose tested in NHPs was below a dose found to be safe in mice. The study lasted for 21 days post-drug administration. Blood samples were collected sequentially for complete blood counts (CBCs), cytokines, PK, PD, and metabolomic studies. Vital signs (weight, temperature, heart rate, and blood pressure) were also measured throughout the study period. The blood collection schedule and overall experimental design are depicted in Fig. 1.

Animals

A total of 12 naïve rhesus macaques (*Macaca mulatta*), six males and six females, 42–71 months of age, weighing 4.1–8.0 kg, were quarantined for 35 days prior to initiation of the study. All animals met the pre-screening requirements before they were shipped to the testing facility for inclusion in the study. Animal quarantine, exclusion criteria, housing, health monitoring, care, and enrichment during the experimental period have been described in detail earlier (*53–55*). Animals were stratified by gender and body weight increases during the quarantine period using Provantis software (Philadelphia, PA) and then assigned to different treatment groups. All rhesus macaques were given unique tattoo identification numbers. This distinctive four-digit number was used in the study data collection systems. All procedures involving animals were approved by the Institutional Animal Care and Use Committee (Southern Research Institute #19-10-047F) and the Department of Defense Animal Care and Use Review Office (ACURO). This study was carried out in accordance with the recommendations provided in the Guide for the Care and Use of Laboratory Animals (*56*).

Cage-side Animal Observations

Animals were observed a minimum of twice per day (morning and afternoon rounds) for the entirety of the quarantine and study periods (*57*). No adverse reactions were observed during this study.

Drug Preparation and Administration

On the afternoon of the day prior to the scheduled dosing day, the BBT-059 container was transferred from –70°C frozen storage to a refrigerator to maintain 2–8°C, and was allowed to thaw overnight. The next day, the thawed drug container was removed from the refrigerator, mixed by gentle inversion 10 times, and kept on wet ice prior to dosing.

Animals were weighed two days before drug administration to determine the volume of drug to be administered to each animal. The

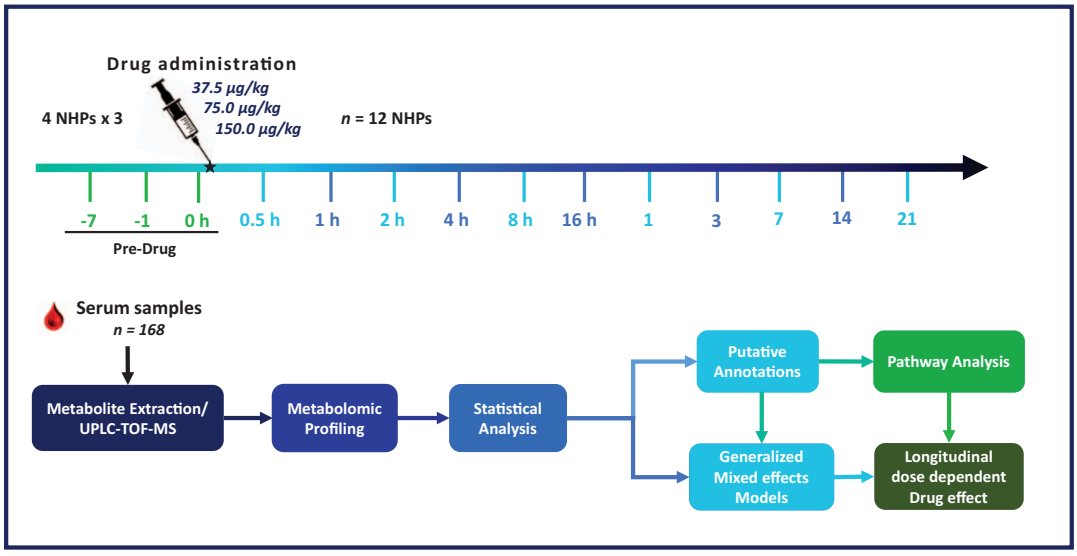

FIG. 1. Experimental design of the NHP study to investigate the impact of BBT-059 administration on serum metabolomics.

injection site preparation and other processes have been discussed earlier (*45*). BBT-059 was then administered by SC injection into the upper back between the shoulder blades. All injection sites were monitored for any signs of reaction or irritation for 24 h.

Vital Signs

Vital signs including heart rate (via pulse oximetry or palpation), blood pressure, temperature, and weight were collected at varying blood collection timepoints as described in detail earlier (*58*). For blood collection, NHPs were restrained in a chair using the pole and collar technique to avoid repeated sedation. Under such situation, it was not practicable to measure the respiratory rate of the NHPs.

Blood Sample Collection

Blood was collected from a peripheral vessel (either saphenous or cephalic vein) as described earlier (*59*). The desired volume of blood was collected with a 3 ml disposable luer-lock syringe with a 25-gauge needle. Whole blood collected in ethylenediaminetetraacetic acid (EDTA) blood collection tubes (Sarstedt Inc., Newton, NC) was used for CBC and for PK analysis, and serum separator tubes (Becton-Dickinson, Franklin Lakes, NJ) were used to collect blood for PD analysis.

Hematology (CBC) Analysis

Approximately 0.5 ml of blood was collected into EDTA tubes for CBC counts and was tested using a Heska Element HT5 hematology analyzer (Colorado, DEA). Parameters evaluated include white blood cell count, red blood cell count, hemoglobin, and hematocrit in addition to platelet, neutrophil, lymphocyte, monocyte, eosinophil, and basophil counts (*60*). CBC analysis was performed for 14 timepoints in total; day –7, day –1 and 0 h prior to drug administration, and 4 h, days 1–7, 10, 14, and 21 post-drug administration.

Multiplex Analysis of Cytokines

A Luminex 200 analyzer (Luminex Corp, Austin, TX) was used to detect the cytokines, chemokines, and growth factors in the serum using custom-made 48-plex multiplex kits (Bio-Rad Laboratories, Hercules, CA). A list of these 48 cytokines has been mentioned earlier (*61*). Standard curves for each cytokine were prepared by serial dilution and run in duplicates. Cytokine concentration (pg/ml) was determined by fluorescence intensity and its quantification was performed using Bio-Plex Manager software, version 6.1 (Bio-Rad Inc.).

PK Analysis

Bioanalysis of plasma samples to measure BBT-059 concentrations was performed using a commercially available ELISA, RayBio Human IL-11 ELISA (RayBiotech, ELH-IL-11, Peachtree Corners, GA), a sandwich-based ELISA assay. As previously stated, four animals (n = 4) were administered one of the three doses (37.5, 75 or 150 µg/kg). Whole blood samples were collected into EDTA tubes prior to drug administration on day –7 and at 0 h, and samples collected at 0.25, 0.5, 1, 2, 4, 8 and 16 h, and on days 1, 3, 7, 14 and 21 were used to assess the concentration of the drug over time (168 samples total). The tubes were inverted slowly 8–10 times, and were then placed on a rocker. Once samples were adequately mixed, samples were centrifuged, and plasma was carefully isolated from the whole blood layer. Samples were stored frozen at –70°C.

The BBT-059 standards of 200 ng/ml to 0.82 ng/ml were prepared by threefold serial dilutions of BBT-059, and were prepared fresh on the day of the assay in 5% rhesus NHP plasma (Cat. No. 028-APEK2-PMG, Biochemed, Winchester, VA) in assay diluent A (supplied with the ELISA kit). The 0 ng/ml standard was 5% rhesus NHP plasma in assay diluent A. Test samples from the study were diluted at least 20 fold into assay diluent A and all subsequent threefold serial dilutions were performed in 5% rhesus NHP plasma in assay diluent A. The ELISA contains an antibody specific for human IL-11 pre-coated onto a 96 well microplate. BBT-059 standards and BBT-059 test samples were measured into the wells in duplicate, incubated at room temperature for 2.5 h with gentle shaking, and any BBT-059 that was present was bound by the immobilized antibody. After washing away any unbound substances, a biotinylated anti-human IL-11 antibody was added to the wells and incubated at room temperature for 1 h with gentle shaking. Plates were washed to remove unbound biotinylated antibody. Horseradish peroxidase-conjugated streptavidin was added to the wells and incubated at room temperature for 45 min with gentle shaking. The wells were again washed, and then TMB (3,3′,5,5′ tetramethylbenzidine) substrate solution was added to the wells for 30 min. Color develops in proportion to the amount of BBT-059 bound in the initial incubation step. The color development was stopped and the intensity of the color was measured at 450 nm with a Molecular Devices Versamax Plate Reader with SoftMax Pro 5.4.1 software (San Jose, CA). The absorbance values for the duplicate BBT-059 standards and test samples were averaged. The software, SoftMax Pro 5.4.1, created a standard curve using a 4-parameter logistic fit, and then determined the concentration of each BBT-059 test sample using this standard curve. The calculated concentration of each BBT-059 test sample was then multiplied by the appropriate dilution factor for the final calculated

BBT-059 concentration. Pharmacokinetic parameters were estimated using Phoenix 64 WinNonlin pharmacokinetic software Build 8.1.0.3530 (Certara L.P.). A non-compartmental approach consistent with the subcutaneous route of administration was used for parameter estimation. The area under the protein concentration versus time curve ($AUC_{(0\text{-}t)}$), $AUC_{(0\text{-}t)}$ divided by the dose administered ($AUC_{(0\text{-}t)}/D$), the area under the concentration versus time curve from time zero to infinity ($AUC_{(0\text{-}\infty)}$), $AUC_{(0\text{-}\infty)}$ divided by the dose administered ($AUC_{(0\text{-}\infty)}/D$), the maximum systemic drug concentration (C_{max}), time to peak plasma concentration (T_{max}), and the half-life ($T_{1/2}$) of the drug were calculated by the WinNonlin program.

Serum Metabolomics using Ultra-High-Performance Liquid Chromatography with Quadrupole Time-of-Flight Mass Spectrometry (UPLC QTOF MS) Analysis

Whole blood was collected in a serum separator tube on day –7, day –1, and at 0 h to determine the baseline concentrations of serum metabolites, at 0.5, 1, 2, 4, 16 h, and on days 1, 3, 7, 14, and 21. Upon sample collection, blood was allowed to clot for a minimum of 30 min. The tube was then placed in a centrifuge to separate the serum. The serum was removed from the tube and placed in a cryogenic storage tube and stored at −80°C until analysis. Metabolite extraction and analysis using UPLC QTOF MS are described in detail earlier (*45*, *62*).

Data Processing and Statistical Analysis

For vital signs, CBC, and cytokine data, mean values with standard errors were reported. One-way analysis of variance (ANOVA) with a Tukey post-hoc test was used to detect significant differences between treatment groups at each timepoint. Additionally, repeated measures two-way ANOVA tests with Bonferroni corrections were also performed for vital signs, CBC, and cytokine data to assess the effects of drug administration over the course of the study within each treatment group. The baseline, which was established by averaging the pre-drug administration timepoints (days –7, –1, and 0 h), was compared to post drug administration timepoints to assess significant differences over time within treatment groups. Statistical software SPSS version 22 (IBM, Armonk, NY) was used for all statistical analyses, and P values less than 0.05 were considered statistically significant.

For metabolomics, data were log transformed and scaled following feature detection; statistical comparisons were performed to follow longitudinal changes in metabolomic profiles and their possible impact on the phenotype. Untargeted metabolomic raw data files were first converted to the NetCDF file format using the Databridge tool in MassLynx (Waters Corporation, Milford, MA). All parameters for peak picking were optimized by IPO (*63*) (Isotopologue Parameter Optimization) R package then processed by XCMS (*64*) package. Data was normalized based on the internal standard and QC-RLSC (QC robust LOESS signal correction (*65*)). Other details of data analysis are described earlier (*45*).

RESULTS

In this study, vital signs, CBC, cytokine, PK/PD, and metabolomic data were analyzed to assess the overall safety and toxicity profile of BBT-059. No adverse reactions to drug administration were noted in any of the treatment groups. Additionally, no treatment-related adverse effects on any of the animals were noted.

BBT-059 Administration Showed Minimal Effects on Vital Signs

Vital signs of each animal were also recorded on blood collection days. All groups generally followed similar trends in vital signs parameters throughout the study. Minimal significant differences were observed between different dose groups at each timepoint in any of the vital sign parameters (body temperature, heart rate, body weight, systolic and diastolic blood pressure) analyzed. Similarly, minimal significant differences were noted when comparing pre-drug administration timepoints to post drug administration timepoints within each treatment group. This suggests that within the dose ranges studied, the drug may not have a significant effect on the vital signs of the subjects, pointing towards a potential acceptable safety profile of BBT-059 at these doses. To provide a visual representation of these data, figures for vital signs data are presented in Supplementary Fig. S1; https://doi.org/10.1667/RADE-23-00194.1.S1[3].

BBT-059 Increased Platelet and Neutrophil Counts

Various samples were collected from a total of 12 animals (n = 4; 37.5, 75 and 150 μg/kg) throughout the course of the study and were analyzed. CBC samples were analyzed starting seven days prior to drug administration and continued until 21 days post-drug administration. The graphs for CBC parameters, including platelet and neutrophil counts, are presented in Supplementary Figs. S2 and S3 (https://doi.org/10.1667/RADE-23-00194.1.S1). BBT-059 administration stimulated some notable changes in CBC counts. Each treatment group generally followed similar trends throughout the course of the study. Platelet counts increased beginning on day 4 in all treatment groups, peaked between days 7 to 10, and decreased toward pre-administration levels by the end of the study. For neutrophils, counts sharply increased within the first 24 h after BBT-059 administration in all groups, and decreased to pre-administration levels by the end of the study. There were some changes in other cell types, such as a drop in lymphocytes and an elevation in monocytes at some timepoints with the highest dose of BBT-059 compared with normal range (*66*). The lymphocyte changes we observed were dose dependent, which suggests the lymphocyte decrease was drug related. When comparing between treatment groups at different timepoints, isolated instances of significance were noted. Monocyte counts were consistently higher for the most part in the 150 μg/kg treatment group, and many of these instances were significant. Additional comparisons were performed to assess significant differences between pre-drug administration timepoints and post drug administration timepoints within the three treatment groups. Significant decreases in RBC, HGB, and HCT% were noted in all three treatment groups at various timepoints, while platelet counts were significantly increased in all treatment groups at various timepoints post drug administration. For all parameters analyzed, post drug administration counts were generally not significantly different when

[3] Editor's note. The online version of this article (DOI: https://doi.org/10.1667/RADE-23-00194.1) contains supplementary information that is available to all authorized users.

comparing to pre-drug administration counts in each treatment group by the end of the study.

Cytokine Response to BBT-059 Administration

Similar to CBC results, cytokine concentrations typically followed similar trends between treatment groups throughout the study. Some notable cytokines including IL-16 and tumor necrosis factor-α (TNF-α) showed an earlier increase in concentration related to BBT-059 administration, with the concentrations in all groups increasing beginning 0.5 h post-administration and lasting through day 1. Increases in concentrations of other cytokines including granulocyte colony-stimulating factor (G-CSF), IL-4, stromal cell-derived factor-1α (SDF-1α, also known as C-X-C motif chemokine 12), and IL-9 were noted later in the study, beginning on days 1, 3 or 7 and lasting throughout the 21-day period. When comparing between treatment groups at different timepoints, significant differences were noted in several cytokines; however, the trends in concentrations mimicked similar patterns over the course of the study in all treatment groups, and the concentrations of one treatment group were not consistently higher or lower than the others. Additional comparisons were performed to assess significance within treatment groups. Significant increases in concentrations of TNF-α, TNF-β, IL-4, IL-9, SCF, and SDF-1α were observed when comparing post drug administration timepoints to the pre-drug administration timepoints within treatment groups, indicating that BBT-059 administration stimulated these responses. To illustrate these observations, figures displaying the cytokine concentrations throughout the study are included in Supplementary Figs. S4–S6 (https://doi.org/10.1667/RADE-23-00194.1.S1). These figures allow for a clear and comprehensive understanding of the temporal cytokine response patterns post-BBT-059 administration, thereby serving as a valuable resource for evaluating the immunomodulatory effects of the drug.

BBT-059 Displayed Dose-Dependent PK Parameters

PK analysis of plasma samples demonstrated that plasma concentrations of BBT-059 were highest within the 24 h period after drug administration, and gradually declined thereafter (Fig. 2). An increased dose of BBT-059 was associated with an increased C_{max}, increased AUC, and increased terminal half-life of the drug. Greater similarities between the 37.5 and 75 μg/kg groups were noted when compared to the 150 μg/kg group. For example, the plasma concentration time profiles [$AUC_{(0\text{-}t)}$ and $AUC_{(0\text{-}inf)}$] were proportional in the 37.5 and 75 μg/kg groups, but supra-proportional to the 150 μg/kg group. When divided by dose, $AUC_{(0\text{-}t)}/D$ and $AUC_{(0\text{-}inf)}/D$ were similar in the 37.5 and 75 μg/kg groups, but nearly two-fold higher in 150 μg/kg group, suggesting a supra-proportional increase in AUC with BBT-059 doses greater than 75 μg/kg. The observed maximum plasma concentration of the drug, known as C_{max}, was consistently increased with higher

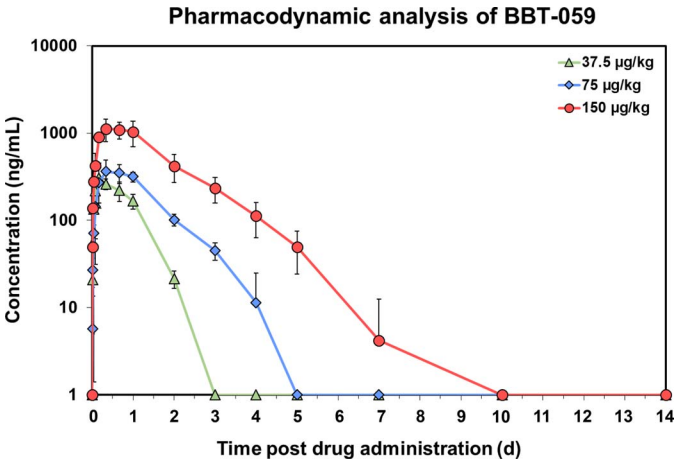

FIG. 2. Pharmacokinetic analysis to assess the concentration of BBT-059 over time (37.5 μg/kg, 75 μg/kg and 150 μg/kg). Data are means ± standard deviations for 4 animals per group.

doses of the drug. Lastly, it was found that T_{max} occurred earlier in the 37.5 μg/kg group compared to the 75 and 150 μg/kg groups. Sex-specific differences were unable to be determined due to the small number of animals in each treatment group (2 males and 2 females per dose). A summary of each of these parameters for each group can be viewed in Table 1.

It is important to note that the 0 ng/ml BBT-059 standard, the pre-drug exposed NHP plasma samples, and late time point NHP plasma samples were negative for BBT-059 (below the limit of quantification). The ELISA kit used in this study could not distinguish between human IL-11 and BBT-059 except for sensitivity. Human and NHP IL-11 share 94% amino acid homology (*67*). Therefore, it is likely NHP IL-11 could have been detected by the human IL-11 ELISA kit used in this study. Plasma samples determined to contain BBT-059 could be measuring a combination of BBT-059 and endogenous NHP IL-11. Therefore, plasma samples determined to be below the lower limit of quantification of BBT-059 are probably also below the lower limit of detection of NHP IL-11.

BBT-059 Administration Stimulated Acute Changes in Serum Metabolomic Profiles that Returned to Pre-Administration Levels by the End of the Study Period

Untargeted metabolomics was performed on the 168 serum samples collected both pre- and post-drug administration from each of the three dose groups. A total of 2,113 and 763 features were detected in the positive and negative electrospray ionization (ESI) modes, respectively. Principal component analysis (PCA) was performed to evaluate the differences between the serum metabolomic profiles before and after drug administration for each treatment group. Metabolomic profiles were compared for each dose group following drug administration to assess dose-dependent changes induced by BBT-059 administration as compared to baseline abundance. A comprehensive list of all

TABLE 1
Summary of BBT-059 Single Dose PK Parameters in NHPs[a]

Dose	Animals	T_{max} (h)	C_{max} (ng/mL)	$AUC_{(0\text{-}t)}$ (ng h/ml)	$AUC_{(0\text{-}inf)}$ (ng h/ml)	$T_{1/2}$ (h)
37.5 µg/kg	All	6 ± 2	330 ± 120	7,608 ± 1,484	7,922 ± 1,442	9.8 ± 2.0
	Males	6 ± 2	287 ± 50	7,037 ± 870	7,459 ± 905	11.4 ± 0.8
	Females	6 ± 2	373 ± 124	8,180 ± 1,376	8,385 ± 1,368	8.2 ± 0.5
75 µg/kg	All	14 ± 8	389 ± 100	14,526 ± 3,060	15,386 ± 2,851	18.2 ± 2.7
	Males	16 ± 8	365 ± 72	13,033 ± 1,162	14,126 ± 709	17.0 ± 2.7
	Females	12 ± 4	413 ± 92	16,018 ± 2,870	16,646 ± 2,918	19.3 ± 0.9
150 µg/kg	All	14 ± 4	1,144 ± 316	55,189 ± 16,327	56,167 ± 16,050	21.2 ± 1.0
	Males	12 ± 4	1,241 ± 283	64,362 ± 13,856	65,270 ± 13,450	21.7 ± 0.7
	Females	16 ± 0	1,048 ± 225	46,016 ± 6,291	47,065 ± 6,306	20.7 ± 0.8

[a] Data are means ± SD for 4 animals per group for all animals (2 males, 2 females) and means ± SEM for 2 animals per group for males and females separately.

metabolites screened in this study can be viewed in Supplementary Table S1 (https://doi.org/10.1667/RADE-23-00194.1.S2). Additionally, comprehensive metabolite and pathway analysis data for each treatment group can be viewed in Supplementary Tables S2–S7.

Overall, BBT-059 generally induced acute changes in metabolomic profiles after administration which fluctuated throughout the study, before returning to near baseline levels by the end of the 21-day study period. Volcano plots were also constructed based on peak intensities of each metabolite for each dose to view additional metabolomic changes induced by BBT-059. The administration of BBT-059 induced early, modest upregulation in metabolomic profiles in all treatment groups. For the early hourly timepoints, the majority of significant metabolites were upregulated, which peaked at around the 4-h timepoint for the 75 and 150 µg/kg treatment groups, and then shifted to majority downregulated. Interestingly, the period of significant upregulation lasted longer for the 37.5 µg/kg group up until the 16 h timepoint. By day 1, the majority of all treatment groups experienced significant downregulation. This pattern of upregulation and downregulation can be viewed in the volcano plots in Fig. 3, which exhibit the 4 h and day 1 timepoints compared to the pre-drug administration timepoints in each treatment group.

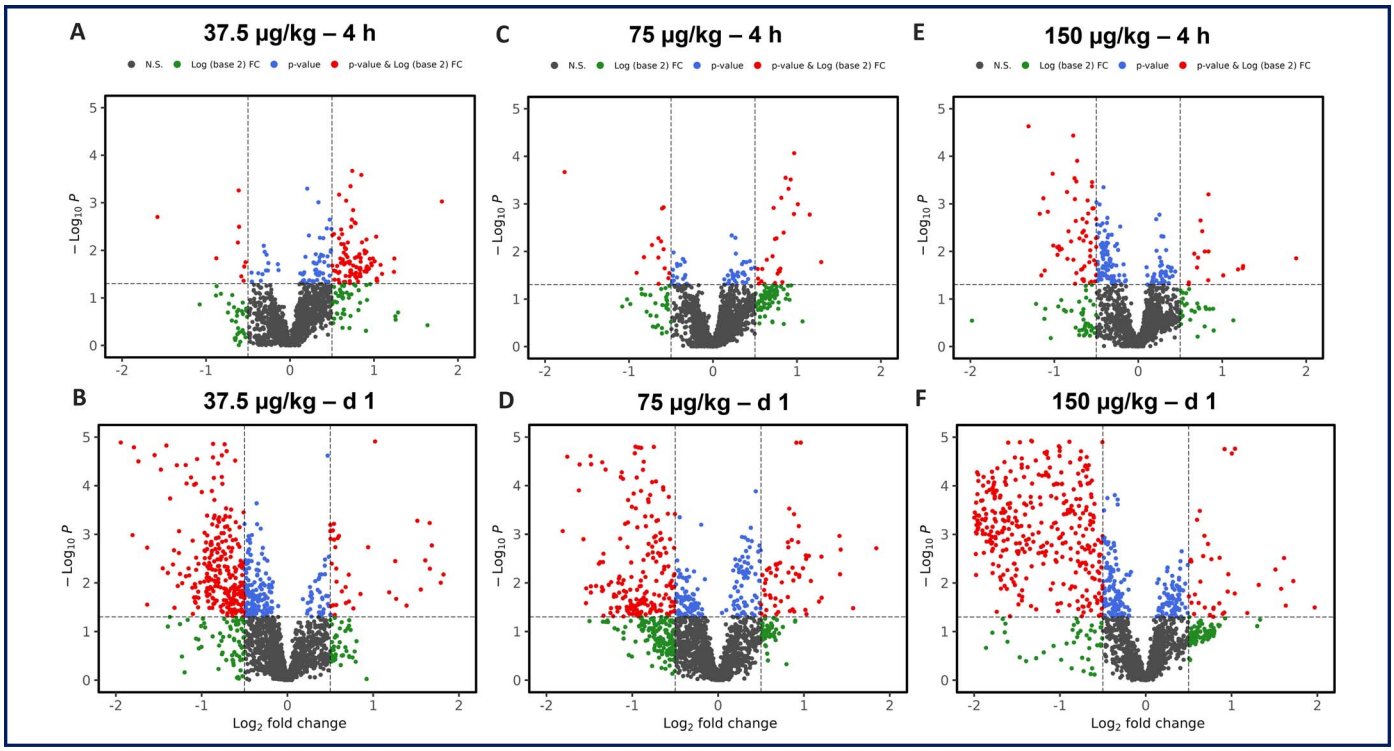

FIG. 3. Volcano plots displaying significant metabolites at 4 h and day 1 post-drug administration compared to the pre-drug administration timepoints: 37.5 µg/kg (panels A and B), 75 µg/kg (panels C and D), and 150 µg/kg groups (panels E and F).

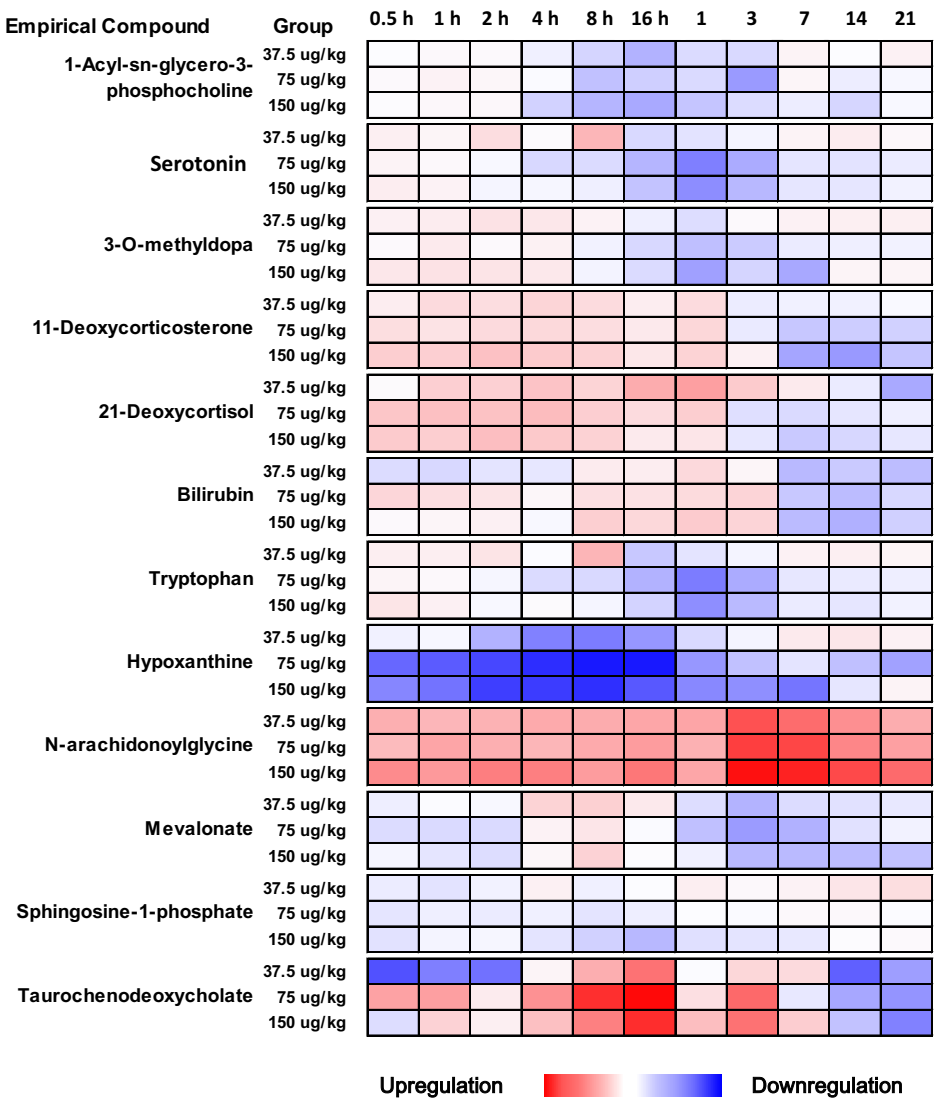

FIG. 4. Heat map displaying the fold change of twelve notable metabolites throughout the course of the study.

Changes in a number of notable metabolites were consistently significant throughout the course of this study. Mevalonate was significantly downregulated for a majority of timepoints in all treatment groups, regardless of treatment group. Metabolites including 11-deoxycorticosterone and 21-deoxycortisol were consistently upregulated in all treatment groups until about day 3 to 7, where these metabolites shifted to downregulation. One metabolite, namely 2-Acetyl-1-alkyl-sn-glycero-3-phosphocholine, was significantly downregulated from the 4-h timepoint through the end of the study period. A few metabolites were only significant in two of the three treatment groups, or were significant in only one group. Two metabolites were significant at eight or more timepoints in the 75 μg/kg treatment group, including tryptophan and serotonin. Similarly, the group treated with 150 μg/kg also had two metabolites that were significant on at least eight timepoints, including 3-O-methyldopa, and sphingosine-1-phosphate. A heat map depicting the fold change of notable metabolites can be seen in Fig. 4.

Metabolic pathways related to inflammation, steroid hormone biosynthesis, and amino acid metabolism were stimulated by the administration of BBT-059, regardless of dose. Several pathways were commonly activated among all three treatment groups including the tyrosine metabolism, squalene and cholesterol biosynthesis, C21-steroid hormone biosynthesis and metabolism, and valine, leucine and isoleucine degradation pathways (Fig. 5). A few pathways were also commonly significantly activated in two of the three treatment groups. For example, the bile acid biosynthesis and vitamin D3 (cholecalciferol) metabolism pathways were significantly activated in the 37.5 and 75 μg/kg treatment groups. Tyrosine metabolism was commonly activated in the 37.5 and 150 μg/kg treatment groups, while porphyrin metabolism was commonly activated in the 75 and 150 μg/kg treatment groups.

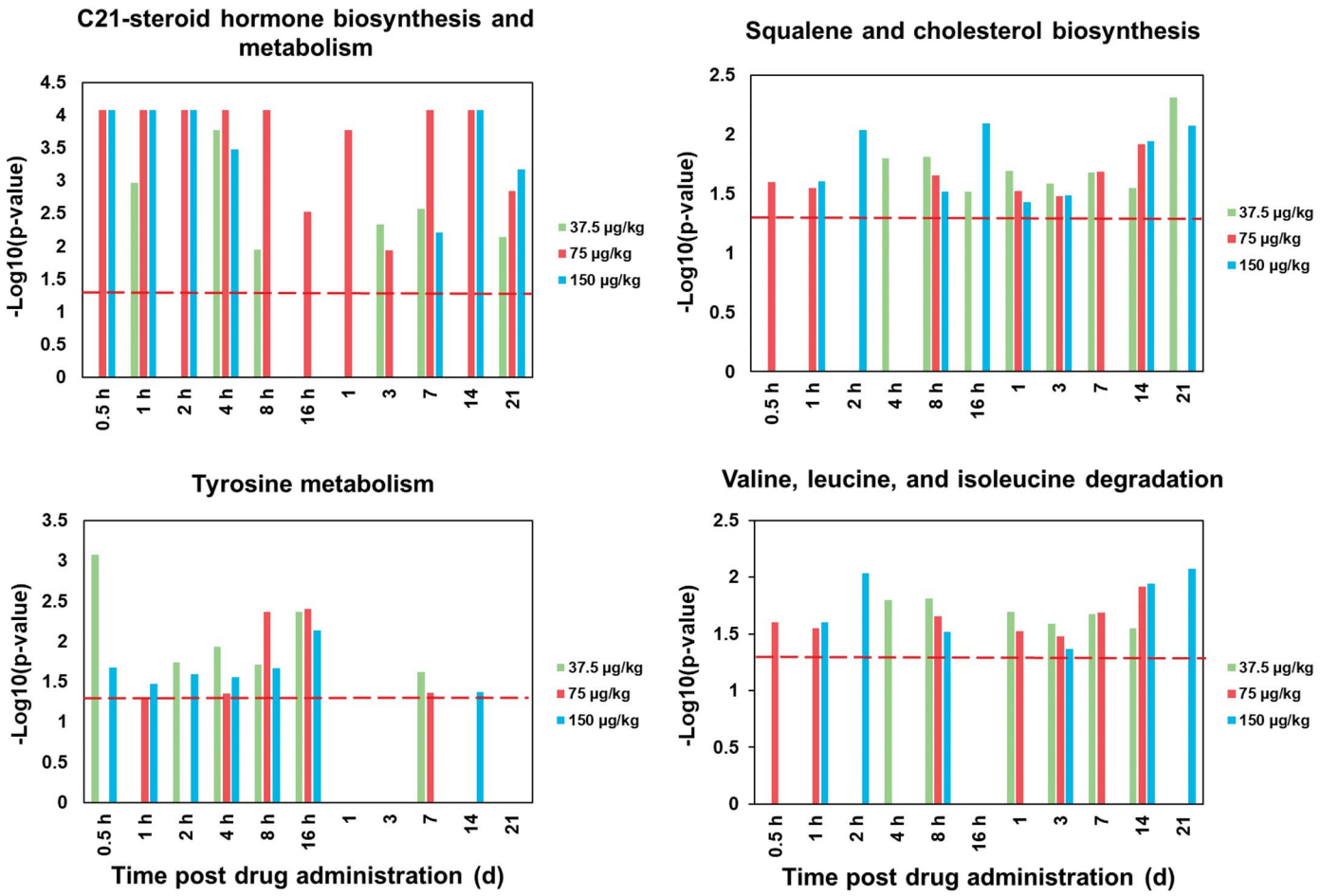

FIG. 5. Significance of key metabolic pathways stimulated by the administration of BBT-059 in the 37.5, 75, and 150 µg/kg treatment groups compared to the pre-drug administration timepoints (day –7, –1, and 0 h).

The administration of 37.5 µg/kg was found to have the greatest influence on squalene and cholesterol biosynthesis, which was significantly activated in 8 of the 11 time points compared to pre-treatment values. The bile acid biosynthesis, vitamin D3 metabolism, and Omega-6 fatty acid metabolism pathways were also notably affected. The 75 µg/kg group was similarly affected, with the C21-steroid hormone biosynthesis and metabolism pathway significantly activated at all timepoints. Porphyrin metabolism, squalene and cholesterol biosynthesis, and valine, leucine, and isoleucine degradation pathways were also significantly activated at several timepoints in the 75 µg/kg group throughout the study. Arachidonic acid metabolism was uniquely activated in this treatment group, and was not affected by administration of the other doses. Similar to the 37.5 µg/kg group, the animals administered 150 µg/kg had the greatest perturbations in squalene and cholesterol biosynthesis.

DISCUSSION

Metabolomic studies provide key insight into radiation damage that occurs at the cellular level, which helps to understand the effects and nature of radiation exposure. We have previously evaluated metabolic changes in serum and tissue samples of both murine (*41–43*) and NHP (*45–49*, *68–72*) models exposed to cobalt-60 total-body gamma-irradiation. These studies suggest that alterations in metabolites induced by acute exposure to lethal doses of gamma radiation can be mitigated to some extent by an MCM. We have also studied a multiplatform metabolomics [LCMS and nuclear magnetic resonance (NMR)] to comprehensively characterize the temporal changes in metabolite levels from mice and NHP samples after γ irradiation, which suggested a unique physiological change that is independent of radiation dose or species (*41*). Additionally, other studies with BIO 300 (*45*, *46*) and gamma tocotrienol (*49*) have been performed in an NHP model where radiation was not used. These studies demonstrated transient metabolic changes as a result of drug administration, which reverted back to pre-drug exposure levels in due course of time. BBT-059 has been found to stimulate the production of platelets, red blood cells and to a lesser extent neutrophils in irradiated mice, and is believed to bring about its biological effects by binding and activating the IL-11 receptors on cells, which may be important for improving survival after lethal irradiation (*37*, *38*).

Overall, PK/PD analysis revealed greater similarities between the 37.5 and 75 μg/kg groups compared to the 150 μg/kg group. The terminal half-life, C_{max}, AUC $_{(0\text{-}t)}$, and AUC $_{(0\text{-}inf)}$ increased with increasing doses of BBT-059. The values of AUC $_{(0\text{-}t)}$ and AUC $_{(0\text{-}inf)}$ were proportional to dose in the 37.5 and 75 μg/kg groups but supra-proportional to dose in the 150 μg/kg group. The values of AUC $_{(0\text{-}t)}$/D and AUC $_{(0\text{-}inf)}$/D were similar in the 37.5 and 75 μg/kg groups, but nearly two-fold higher in 150 μg/kg group, suggesting a supra-proportional increase in AUC with BBT-059 doses greater than 75 μg/kg. The value of V_z/F suggests that BBT-059 is largely confined to the blood/plasma compartment. Lastly, T_{max} occurred earlier in the 37.5 μg/kg group compared to the 75 and 150 μg/kg groups. Additionally, the administration of BBT-059 was found to have a positive effect on hematopoiesis, stimulating the production of platelets and neutrophils. BBT-059 administration also had significant effects on serum cytokine induction, with changes in IL-16, TNF-α, G-CSF, TNF-β, IL-9, SCF, and SDF-1α concentrations. We have also performed repeated measures two-way ANOVA tests with Bonferroni corrections that compared the average of the pre-drug administration timepoints (days –7, –1 and 0 h) to the post-drug administration timepoints for each treatment group. The results of these comprehensive statistical comparisons for vital signs, CBC, and cytokine data are included in Supplementary Tables S8–S10, respectively (https://doi.org/10.1667/RADE-23-00194.1.S2), to demonstrate that no toxicity was observed. Interestingly, administration of exogenous G-CSF after radiation exposure is associated with decreased periods of neutropenia, a reduced infection risk, and enhanced bone marrow recovery in clinical case studies, suggesting that this cytokine plays an important role in the radioprotective mechanism (*73*). Overall, biomarker discovery is a key part of drug development, as robust and validated biomarkers can be used to guide dose adjustments and determine safety profiles, and provide valuable insight into how a drug provides its intended effect.

As for BBT-059's effects on metabolomics, fluctuations in several metabolites and metabolic pathways were stimulated by BBT-059 administration. A few notable metabolites related to steroid hormone biosynthesis pathways were significantly stimulated in all treatment groups throughout the study, including 21-deoxycortisol, 11-deoxycorticosterone, and mevalonate. Bilirubin, which has cytoprotective and anti-inflammatory effects, was significantly upregulated for a few timepoints in all treatment groups beginning about 1 day after drug administration, but was then downregulated and returned to near pre-exposure levels by the end of the 21 day study (*74*). Phosphatidylcholine, which fluctuated slightly in all treatment groups before returning to near pre-exposure levels, plays a key role in regulating the structural properties of cellular membranes. Interestingly, an absence of phosphatidylcholine in intestinal mucosa has been linked to an increase of colonic bacteria, which can result in intestinal inflammation and a compromised intestinal barrier (*75*). All of the above metabolites are known to reduce inflammation, which could provide insight into how BBT-059 exerts its radioprotective effects. Radiation is known to induce inflammation in many organs and organ systems, including the lungs and GI system.

BBT-059 also significantly stimulated the expression of a few unique metabolites, or metabolites that were isolated to a single treatment group. Tryptophan and serotonin, which are involved in the modulation of immune responses, were both significantly upregulated and downregulated at various timepoints in the 75 μg/kg treatment group. Sphingosine-1-phosphate, which was uniquely downregulated in the 150 μg/kg treatment group, is a potent cell signaling molecule known as a lipid mediator, and is associated with immune cell trafficking from the lymphoid organs into circulation (*76*).

Overall, BBT-059 administration mostly stimulated the same pathways across all dose groups, apart from a few exceptions. Two of the most significantly affected pathways among the three BBT-059 dosing groups was the C-21 steroid hormone biosynthesis and metabolism pathway and the squalene and cholesterol biosynthesis pathway. A few pathways involved in amino acid metabolism were significantly activated throughout the course of the study, including tyrosine metabolism, valine, leucine and isoleucine degradation, and urea cycle/amino group metabolism. Tyrosine phosphorylation is an important mechanism for the regulation of many physiological processes, with both inhibitory and excitatory effects in the immune response (*77*). Stimulation of these pathways by BBT-059 administration suggests that this drug has anti-inflammatory properties, which make it a promising candidate for countering radiation injury.

It is important to note that there are certain limitations in this study. This study was performed with a total of 12 NHPs; four NHPs (2 males and 2 females) in each dose group. However, this sample size is realistically too small to identify any sex-related differences. For all of the analyses, male and female samples were pooled, and this should be considered a mixed sex study. It is also important to note that we have recently demonstrated that under matched experimental conditions, there is clearly evident differences between acutely irradiated male and female NHPs relative to the measured response endpoints (survival rates, blood cell changes and cytokine fluctuations) (*78*). Such differences were accentuated by the level of radiation exposure and nature of clinical support. The length of the PK study window for this study was 21 days, which is similar to other PK studies. However, this time window can be shorter depending on the drug under test. We have accomplished several such studies with various MCMs using a time window of 21 days or less (*45*, *46*, *53*). Additionally, these NHPs were reused in another study after a few months and they displayed no obvious adverse effects at the time the other study was initiated. Though we expect

all of the changes are due to the drug, it is possible that some minor immune changes may be due to the injection.

In brief, the results of this current study suggest that the administration of BBT-059 at 37.5, 75 and 150 μg/kg are well tolerated and are free from any adverse effects. BBT-059 administration stimulated several metabolic pathways related to steroid hormone biosynthesis and metabolism as well as amino acid metabolism. While the higher dose of 150 μg/kg did not display signs of toxicity, the PK analysis suggests that doses greater than 75 μg/kg result in supra-proportional increases in AUC without additional physiological benefit. For this reason, the 37.5 and 75 μg/kg BBT-059 doses seem most promising and warrant further investigation into their efficacy against ionizing radiation in NHPs.

ACKNOWLEDGMENTS

The authors would like to thank the staff of the Southern Research Institute for animal care; and the staff of the Radiation Science Department, AFRRI, for dosimetry and radiation exposure to the animals. We also thank Ms. Brianna L. Janocha for help in data analysis and Dr. Carmen Rios and Dr. Andrea L. Dicarlo-Cohen for scientific discussions. The authors would like to acknowledge the Metabolomics Shared Resource in Georgetown University (Washington, DC) partially supported by NIH/NCI/CCSG grant P30-CA051008. The authors gratefully acknowledge the research support from the National Institute of Allergy and Infectious Diseases (AAI12044-001-07000 - Work plan G) as Interagency-Agreements, and the Uniformed Services University of the Health Sciences/Armed Forces Radiobiology Research Institute (grant no. AFR-10978 and 12080) to VKS. All procedures were approved by AFRRI, Southern Research Institute (SR), and Department of Defense Animal Care and Use Review Office (ACURO). This study was carried out in strict accordance with the Guide for the Care and Use of Laboratory Animals of the National Institutes of Health. Data availability, all relevant data are within the manuscript and its Supporting Information files. The opinions or assertions contained herein are the private views of the authors and are not necessarily those of the Uniformed Services University of the Health Sciences, or the Department of Defense. The mention of specific therapeutic agents does not constitute endorsement by the U.S. Department of Defense, and trade names are used only for the purpose of clarification.

Received: September 23, 2023; accepted: April 23, 2024; published online: May 8, 2024

REFERENCES

1. Carter AB, May MM, Perry WJ. The day after: Action following a nuclear blast in a U.S. city. Washington Quarterly 2007; 30: 19-32.
2. Gale RP, Armitage JO. Are we prepared for nuclear terrorism? N Engl J Med 2018; 378:1246-54.
3. Benjamin GC, McGeary M, McCutchen SR. Topic 1: Effects of a 10-kt IND detonation on human health and the area of health care system. A Workshop Report. Washington, D.C.: The National Academies Press; 2009. p. 7-26.
4. Dainiak N, Waselenko JK, Armitage JO, MacVittie TJ, Farese AM. The hematologist and radiation casualties. Hematology: American Society of Hematology Education Program 2003; 2003: 473-96.
5. Weisdorf D, Chao N, Waselenko JK, Dainiak N, Armitage JO, McNiece I, Confer D. Acute radiation injury: contingency planning for triage, supportive care, and transplantation. Biol Blood Marrow Transplant 2006; 12:672-82.
6. Waselenko JK, MacVittie TJ, Blakely WF, Pesik N, Wiley AL, Dickerson WE, et al. Medical management of the acute radiation syndrome: Recommendations of the Strategic National Stockpile Radiation Working Group. Ann Intern Med 2004; 140:1037-51.
7. Dorr H, Meineke V. Acute radiation syndrome caused by accidental radiation exposure - therapeutic principles. BMC Med 2011; 9: 126.
8. McCann DGC. Radiation poisoning: Current concepts in the acute radiation syndrome. Am J Clin Med 2006; 3:13-21.
9. Farese AM, MacVittie TJ. Filgrastim for the treatment of hematopoietic acute radiation syndrome. Drugs Today (Barc) 2015; 51: 537-48.
10. Singh VK, Seed TM. An update on sargramostim for treatment of acute radiation syndrome. Drugs Today (Barc) 2018; 54:679-93.
11. Singh VK, Seed TM. Radiation countermeasures for hematopoietic acute radiation syndrome: growth factors, cytokines and beyond. Int J Radiat Biol 2021; 97:1526-47.
12. Hankey KG, Farese AM, Blaauw EC, Gibbs AM, Smith CP, Katz BP, et al. Pegfilgrastim improves survival of lethally irradiated nonhuman primates. Radiat Res 2015; 183:643-55.
13. Clayton NP, Khan-Malek RC, Dangler CA, Zhang D, Ascah A, Gains M, et al. Sargramostim (rhu GM-CSF) improves survival of non-human primates with severe bone marrow suppression after acute, high-dose, whole-body irradiation. Radiat Res 2021; 195: 191-9.
14. Zhong Y, Pouliot M, Downey AM, Mockbee C, Roychowdhury D, Wierzbicki W, Authier S. Efficacy of delayed administration of sargramostim up to 120 hours post exposure in a nonhuman primate total body radiation model. Int J Radiat Biol 2021; 97: S100-S16.
15. Singh VK, Seed TM. An update on romiplostim for treatment of acute radiation syndrome. Drugs Today (Barc) 2022; 58:133-45.
16. Farese AM, Cohen MV, Katz BP, Smith CP, Gibbs A, Cohen DM, MacVittie TJ. Filgrastim improves survival in lethally irradiated nonhuman primates. Radiat Res 2013; 179:89-100.
17. Lazarus HM, McManus J, Gale RP. Sargramostim in acute radiation syndrome. Expert Opin Biol Ther 2022; 22:1345-52.
18. Wong K, Chang PY, Fielden M, Downey AM, Bunin D, Bakke J, et al. Pharmacodynamics of romiplostim alone and in combination with pegfilgrastim on acute radiation-induced thrombocytopenia and neutropenia in non-human primates. Int J Radiat Biol 2020; 96:155-66.
19. Bunin DI, Javitz HS, Gahagen J, Bakke J, Lane JH, Andrews DA, Chang PY. Survival and hematologic benefits of romiplostim after acute radiation exposure supported FDA approval under the animal rule. Int J Radiat Oncol Biol Phys 2023; 17:705-17.
20. U.S. Food and Drug Administration. Radiological and nuclear emergency preparedness information from FDA. 2023. Available at: https://www.fda.gov/emergency-preparedness-and-response/mcm-issues/radiological-and-nuclear-emergency-preparedness-information-fda [Last accessed 2023].
21. Fresenius Kabi. STIMUFEND (pegfilgrastim-fpgk) is biosimilar* to NEULASTA (pegfilgrastim). 2023. Available at: https://www.fda.gov/media/172679/download?attachment [Last accessed 2023].
22. Coherus BioSciences Inc. UDENYCA (pegfilgrastim-cbqv) is biosimilar* to NEULASTA (pegfilgrastim). 2022. Available at: https://www.accessdata.fda.gov/drugsatfda_docs/label/2022/761039s014lbl.pdf [Last accessed 2023].
23. Singh VK, Garcia M, Seed TM. A review of radiation countermeasures focusing on injury-specific medicinals and regulatory approval status: part II. Countermeasures for limited indications, internalized radionuclides, emesis, late effects, and agents demonstrating efficacy in large animals with or without FDA IND status. Int J Radiat Biol 2017; 93:870-84.
24. Singh VK, Hanlon BK, Santiago PT, Seed TM. A review of radiation countermeasures focusing on injury-specific medicinals and regulatory approval status: part III. Countermeasures under early

stages of development along with 'standard of care' medicinal and procedures not requiring regulatory approval for use. Int J Radiat Biol 2017; 93:885-906.

25. Singh VK, Seed TM. A review of radiation countermeasures focusing on injury-specific medicinals and regulatory approval status: part I. Radiation sub-syndromes, animal models and FDA-approved countermeasures. Int J Radiat Biol 2017; 93: 851-69.

26. Singh VK, Seed TM. Development of gamma-tocotrienol as a radiation medical countermeasure for the acute radiation syndrome: Current status and future perspectives. Expert Opin Investig Drugs 2023; 32:25-35.

27. Singh VK, Seed TM. BIO 300: a promising radiation countermeasure under advanced development for acute radiation syndrome and the delayed effects of acute radiation exposure. Expert Opin Investig Drugs 2020; 29:429-41.

28. Metcalfe RD, Putoczki TL, Griffin MDW. Structural understanding of interleukin 6 family cytokine signaling and targeted therapies: Focus on interleukin 11. Front Immunol 2020; 11:1424.

29. Singh VK, Seed TM. The safety and efficacy of interleukin 11 for radiation injury. Expert Opin Drug Saf 2023; 22:105-9.

30. Dams-Kozlowska H, Gryska K, Kwiatkowska-Borowczyk E, Izycki D, Rose-John S, Mackiewicz A. A designer hyper interleukin 11 (H11) is a biologically active cytokine. BMC Biotechnol 2012; 12:8.

31. Kaye JA. The clinical development of recombinant human interleukin 11 (NEUMEGA rhIL-11 growth factor). Stem Cells 1996; 14 Suppl 1:256-60.

32. Reynolds CH. Clinical efficacy of rhIL-11. Oncology (Williston Park) 2000; 14:32-40.

33. Burnett AF, Biju PG, Lui H, Hauer-Jensen M. Oral interleukin 11 as a countermeasure to lethal total-body irradiation in a murine model. Radiat Res 2013; 180:595-602.

34. Potten CS. Protection of the small intestinal clonogenic stem cells from radiation-induced damage by pretreatment with interleukin 11 also increases murine survival time. Stem Cells 1996; 14: 452-9.

35. Seed TM, Inal CE, Deen JE. Assessment of a combined G-CSF plus IL-11 cytokine treatment for radiation-induced hematopoietic injury. 48th Annual Meeting of the Radiation Research Society. San Juan, Puerto Rico; 2001. p. 161.

36. Hao J, Sun L, Huang H, Xiong G, Liu X, Qiu L, et al. Effects of recombinant human interleukin 11 on thrombocytopenia and neutropenia in irradiated rhesus monkeys. Radiat Res 2004; 162: 157-63.

37. Kumar VP, Biswas S, Sharma NK, Stone S, Fam CM, Cox GN, Ghosh SP. PEGylated IL-11 (BBT-059): A novel radiation countermeasure for hematopoietic acute radiation syndrome. Health Phys 2018; 115:65-76.

38. Plett PA, Chua HL, Sampson CH, Katz BP, Fam CM, Anderson LJ, et al. PEGylated G-CSF (BBT-015), GM-CSF (BBT-007), and IL-11 (BBT-059) analogs enhance survival and hematopoietic cell recovery in a mouse model of the hematopoietic syndrome of the acute radiation syndrome. Health Phys 2014; 106:7-20.

39. Bolder BioTechnology. Pipeline. 2017. Available at: http://www.bolderbio.com/pipeline/ [Last accessed 2023].

40. Tuntland T, Ethell B, Kosaka T, Blasco F, Zang RX, Jain M, et al. Implementation of pharmacokinetic and pharmacodynamic strategies in early research phases of drug discovery and development at Novartis Institute of Biomedical Research. Front Pharmacol 2014; 5:174.

41. Crook A, De Lima Leite A, Payne T, Bhinderwala F, Woods J, Singh VK, Powers R. Radiation exposure induces cross-species temporal metabolic changes that are mitigated in mice by amifostine. Sci Rep 2021; 11:14004.

42. Cheema AK, Li Y, Girgis M, Jayatilake M, Fatanmi OO, Wise SY, et al. Alterations in tissue metabolite profiles with amifostine-prophylaxed mice exposed to gamma radiation. Metabolites 2020; 10:211.

43. Cheema AK, Li Y, Girgis M, Jayatilake M, Simas M, Wise SY, et al. Metabolomic studies in tissues of mice treated with amifostine and exposed to gamma-radiation. Sci Rep 2019; 9:15701.

44. Singh VK, Seed TM. The efficacy and safety of amifostine for the acute radiation syndrome. Expert Opin Drug Saf 2019; 18: 1077-90.

45. Li Y, Girgis M, Jayatilake M, Serebrenik AA, Cheema AK, Kaytor MD, Singh VK. Pharmacokinetic and metabolomic studies with a BIO 300 oral powder formulation in nonhuman primates. Sci Rep 2022; 12:13475.

46. Cheema AK, Mehta KY, Santiago PT, Fatanmi OO, Kaytor MD, Singh VK. Pharmacokinetic and metabolomic studies with BIO 300, a nanosuspension of genistein, in a nonhuman primate model. Int J Mol Sci 2019; 20:1231.

47. Li Y, Girgis M, Wise SY, Fatanmi OO, Seed TM, Maniar M, et al. Analysis of the metabolomic profile in serum of irradiated nonhuman primates treated with Ex-Rad, a radiation countermeasure. Sci Rep 2021; 11:11449.

48. Pannkuk EL, Laiakis EC, Fornace AJ, Jr., Fatanmi OO, Singh VK. A metabolomic serum signature from nonhuman primates treated with a radiation countermeasure, gamma-tocotrienol, and exposed to ionizing radiation. Health Phys 2018; 115:3-11.

49. Cheema AK, Mehta KY, Fatanmi OO, Wise SY, Hinzman CP, Wolff J, Singh VK. A Metabolomic and lipidomic serum signature from nonhuman primates administered with a promising radiation countermeasure, gamma-tocotrienol. Int J Mol Sci 2018; 19:79.

50. Singh VK, Hauer-Jensen M. Gamma-tocotrienol as a promising countermeasure for acute radiation syndrome: Current status. Int J Mol Sci 2016; 17:e663.

51. Singh VK, Olabisi AO. Nonhuman primates as models for the discovery and development of radiation countermeasures. Expert Opin Drug Discov 2017; 12:695-709.

52. U.S. Food and Drug Administration. Guidance for Industry: Estimating the maximum safe starting dose in initial clinical trials for therapeutics in adult healthy volunteers. 2005. Available at: https://www.fda.gov/regulatory-information/search-fda-guidance-documents/estimating-maximum-safe-starting-dose-initial-clinical-trials-therapeutics-adult-healthy-volunteers [Last accessed 2023].

53. Singh VK, Kulkarni S, Fatanmi OO, Wise SY, Newman VL, Romaine PL, et al. Radioprotective efficacy of gamma-tocotrienol in nonhuman primates. Radiat Res 2016; 185:285-98.

54. Li Y, Singh J, Varghese R, Zhang Y, Fatanmi OO, Cheema AK, Singh VK. Transcriptome of rhesus macaque (Macaca mulatta) exposed to total-body irradiation. Sci Rep 2021; 11:6295.

55. Phipps AJ, Bergmann JN, Albrecht MT, Singh VK, Homer MJ. Model for evaluating antimicrobial therapy to prevent life-threatening bacterial infections following exposure to a medically significant radiation dose. Antimicrob Agents Chemother 2022; 66:e0054622.

56. National Research Council of the National Academy of Sciences. Guide for the care and use of laboratory animals. 8th ed. Washington, DC: National Academies Press; 2011.

57. Girgis M, Li Y, Ma J, Sanda M, Wise SY, Fatanmi OO, et al. Comparative proteomic analysis of serum from nonhuman primates administered BIO 300: a promising radiation countermeasure. Sci Rep 2020; 10:19343.

58. Singh VK, Fatanmi OO, Wise SY, Carpenter AD, Olsen CH. Determination of lethality curve for cobalt-60 gamma-radiation source in rhesus macaques using subject-based supportive care. Radiat Res 2022; 198:599-614.

59. Cheema AK, Li Y, Moulton J, Girgis M, Wise SY, Carpenter A, et al. Identification of novel biomarkers for acute radiation injury using multiomics approach and nonhuman primate model. Int J Radiat Oncol Biol Phys 2022; 114:310-20.

60. Garg TK, Garg S, Miousse IR, Wise SY, Carpenter AD, Fatanmi OO, et al. Gamma-tocotrienol modulates total-body irradiation-induced

hematopoietic injury in a nonhuman primate model. Int J Mol Sci 2022; 23.

61. Kulkarni S, Singh PK, Ghosh SP, Posarac A, Singh VK. Granulocyte colony-stimulating factor antibody abrogates radioprotective efficacy of gamma-tocotrienol, a promising radiation countermeasure. Cytokine 2013; 62:278-85.

62. Cheema AK, Li Y, Singh J, Johnson R, Girgis M, Wise SY, et al. Microbiome study in irradiated mice treated with BIO 300, a promising radiation countermeasure. Anim Microbiome 2021; 3:71.

63. Libiseller G, Dvorzak M, Kleb U, Gander E, Eisenberg T, Madeo F, et al. IPO: a tool for automated optimization of XCMS parameters. BMC Bioinformatics 2015; 16:118.

64. Smith CA, Want EJ, O'Maille G, Abagyan R, Siuzdak G. XCMS: processing mass spectrometry data for metabolite profiling using nonlinear peak alignment, matching, and identification. Anal Chem 2006; 78:779-87.

65. Dunn WB, Broadhurst D, Begley P, Zelena E, Francis-McIntyre S, Anderson N, et al. Procedures for large-scale metabolic profiling of serum and plasma using gas chromatography and liquid chromatography coupled to mass spectrometry. Nat Protoc 2011; 6:1060-83.

66. Chen Y, Qin S, Ding Y, Wei L, Zhang J, Li H, et al. Reference values of clinical chemistry and hematology parameters in rhesus monkeys (Macaca mulatta). Xenotransplantation 2009; 16:496-501.

67. Li Y, Wu Q, Jin Y, Yang Q. Antiviral activity of interleukin-11 as a response to porcine epidemic diarrhea virus infection. Vet Res 2019; 50:111.

68. Cheema AK, Hinzman CP, Mehta KY, Hanlon BK, Garcia M, Fatanmi OO, Singh VK. Plasma derived exosomal biomarkers of exposure to ionizing radiation in nonhuman primates. Int J Mol Sci 2018; 19:3427.

69. Pannkuk EL, Laiakis EC, Garcia M, Fornace AJ, Jr., Singh VK. Nonhuman primates with acute radiation syndrome: Results from a global serum metabolomics study after 7.2 Gy total-body irradiation. Radiat Res 2018; 190:576-83.

70. Pannkuk EL, Laiakis EC, Singh VK, Fornace AJ. Lipidomic signatures of nonhuman primates with radiation-induced hematopoietic syndrome. Sci Rep 2017; 7:9777.

71. Cheema AK, Mehta KY, Rajagopal MU, Wise SY, Fatanmi OO, Singh VK. Metabolomic studies of tissue injury in nonhuman primates exposed to gamma-radiation. Int J Mol Sci 2019; 20:3360.

72. Carpenter AD, Li Y, Fatanmi OO, Wise SY, Petrus SA, Janocha BL, et al. Metabolomic profiles in tissues of nonhuman primates exposed to total- or partial-body radiation. Radiat Res 2024; (in press).

73. Reeves G. Overview of use of G-CSF and GM-CSF in the treatment of acute radiation injury. Health Phys 2014; 106:699-703.

74. Vogel ME, Zucker SD. Bilirubin acts as an endogenous regulator of inflammation by disrupting adhesion molecule-mediated leukocyte migration. Inflamm Cell Signal 2016; 3.

75. Stremmel W, Ehehalt R, Staffer S, Stoffels S, Mohr A, Karner M, Braun A. Mucosal Protection by Phosphatidylcholine. Digestive Diseases 2013; 30:85-91.

76. Mendelson K, Evans T, Hla T. Sphingosine 1-phosphate signalling. Development 2014; 141:5-9.

77. Mustelin T, Vang T, Bottini N. Protein tyrosine phosphatases and the immune response. Nat Rev Immunol 2005; 5:43-57.

78. Singh VK, Carpenter AD, Janocha BL, Petrus SA, Fatanmi OO, Wise SY, Seed TM. Radiosensitivity of rhesus nonhuman primates: Consideration of sex, supportive care, body weight and age at time of exposure. Expert Opin Drug Discov 2023; 18:797-814.